Sensors & Actuators: B. Chemical 311 (2020) 127857

Contents lists available at ScienceDirect

Sensors and Actuators B: Chemical

journal homepage: www.elsevier.com/locate/snb

Simultaneous detection of streptomycin and kanamycin based on an all-solid-state potentiometric aptasensor array with a dual-internal calibration system

Juan Yu, Wanxin Tang, Fan Wang, Fan Zhang*, Qingjiang Wang, Pingang He

School of Chemistry and Molecular Engineering, East China Normal University, 500 Dongchuan Road, Shanghai, 200241, PR China

ARTICLE INFO

Keywords:
Aptasensor
Dual-internal calibration
Potentiometry
Streptomycin
Kanamycin

ABSTRACT

A novel potentiometric aptasensor array based on a 4-channel screen-printed carbon electrode was developed with a dual-internal calibration system for the simultaneous detection of streptomycin and kanamycin. Two channels were used as working channels for assembling the aptamers of the two targets, and the other two channels acted as calibration channels. The calibration channels functioned by immobilizing two all-A sequences were employed to subtract the influence from the background matrix and further improve the detection accuracy. Consequently, under optimal conditions, this aptasensor array showed high sensitivity for the detection of streptomycin and kanamycin with detection limits of 9.66 pM and 5.24 pM, respectively, and corresponding linear response ranges of 10 pM–10 μM and 10 pM–1 μM, respectively. Moreover, it presented high specificity without mutual interference between the two targets or with other antibiotics and also demonstrated good repeatability. This aptasensor array was further applied to the simultaneous detection of streptomycin and kanamycin in real milk samples, and the results were validated by liquid chromatography-mass spectrometry (LC–MS). The results demonstrated satisfactory accuracy and precision and showed the great application potential of the aptasensor array with internal calibration for on-site detection of multiple targets.

1. Introduction

Antibiotics are widely used in modern healthcare and livestock husbandry for the treatment of bacterial infections [1]. Streptomycin and kanamycin are both aminoglycoside antibiotics that have broad-spectrum antibacterial effects on many gram-negative bacteria and gram-positive bacteria [2,3]. However, the excessive use and abuse of antibiotics can cause antibiotic residues to be found in human body, which can lead to serious side effects, such as loss of hearing and nephrotoxicity [4,5]. In October 2001, the "Industrial Standard for Pollution-free Foods and Fresh Milk" issued by the Ministry of Agriculture of China stipulated that antibiotics should not be detected in raw milk. Therefore, sensitive, selective, accurate and simple detection methods for monitoring antibiotics in animal-derived foods are in high demand.

At present, the common methods used for detecting antibiotic residues include high-performance liquid chromatography (HPLC) [6,7], liquid chromatography-mass spectrometry (LC–MS) [8,9], immunoassays [10,11], fluorimetry and colorimetry [12–15]. These traditional methods are stable and reliable but most of them require relatively large instruments and cannot be designed as portable devices to achieve on-site detection.

All-solid-state potentiometric sensing based on polymeric membrane ion-selective electrodes (ISEs) was first reported in the 1970s [16]. Since then, it has attracted tremendous attention in recent years because of its simple preparation, portability and easy miniaturization. Traditional ion-selective membrane-based potentiometric sensing mostly conforms to the Nernst response. Recently, with the combination of aptamer as a novel recognition element, potentiometric sensing has been applied to the detection of organic small molecules [17–19], proteins and bacteria [20–22]. However, the responses do not follow the Nernst equation.

Aptamers are considered as ideal recognition elements due to their high specificity and high affinity for binding to targets [23]. Compared with antibodies, aptamers have the advantages of large-scale production, reduced batch-to-batch variability, and easy chemical modification [24]. In potentiometric aptasensing, negatively charged aptamers can combine with targets to form special rigid three-dimensional strcture; the formation of the complex removes aptamers from the electrode surface, resulting in a change in potential [25–27]. That is, potentiometric aptasensing is performed based on the variation of

* Corresponding author.
E-mail address: fzhang@chem.ecnu.edu.cn (F. Zhang).

https://doi.org/10.1016/j.snb.2020.127857
Received 10 October 2019; Received in revised form 7 February 2020; Accepted 10 February 2020
Available online 21 February 2020
0925-4005/

charges on the electrode surface, which is quite different from the Nernst responses. These variations are mainly caused by the recognition event of the target. Moreover, the background matrix of the detection system can also affect the potential of the working electrode. To deduct background interference and further improve the detection accuracy [28,29], our group has developed a potentiometric aptasensor array, which integrates an internal calibration channel, to realize the simultaneous detection of Hg^{2+}, Cd^{2+}, and As^{3+} [30]. On this channel, an all-A sequence with the same length as aptamers is immobilized to provide an internal calibration potential. Since the aptamers of the three target ions have different lengths, the two shorter ones are extended in reference to the longest one, thus obtaining consistent initial potentials of four channels. It is worth noting, however, that the extended aptamer may affect its capability to recognize the target.

In this work, a novel potentiometric aptasensor array is developed with dual-channel internal calibration to simultaneously detect streptomycin and kanamycin using open circuit potential (OCP) technology. Reduced graphene oxide (rGO) is first modified on the electrode as an effective solid contact transducer, and then dendritic gold nanostructure (denAu) is coated to expand the effective area of the electrode and immobilize more aptamers. Two electrodes in the array are fixed with streptomycin and kanamycin aptamers, and the other two are fixed with two all-A sequences, with similar lengths as the corresponding aptamers. Integrating two calibration channels, the detection potentials of kanamycin and streptomycin can be calibrated separately. The binding of the target and the aptamer occurs mainly at some specific bases of the aptamer loop region (“GGGT” for streptomycin and “GG” for kanamycin, Fig. S1) [31,32]. They are folded by hydrogen bonding to form rigid three-dimensional complex, which separate the phosphate groups of the aptamers from the electrode surface; the decrease in the negative charge on the electrode surface induces an increase in the recorded potential. Since the all-A sequences on the calibration channels do not recognize the target, the changes in potential may reflect the influence of the background matrix. Thus, the difference of potentials (ΔOCP) between the working channels and calibration channels can be employed for a simultaneous quantitative analysis of two targets with high sensitivity, specificity and accuracy, thus providing an effective and practical approach for the on-site detection of multiple targets in many fields.

2. Experimental section

2.1. Reagents and materials

Kanamycin, streptomycin, amoxicillin, gentamycin sulfate, chloramphenicol, 6-mercapto-1-hexanol, tetrachloroaurate(III) tetrahydrate ($HAuCl_4{\cdot}4H_2O$, 47.8 % Au), H_2SO_4, HCl, tris(2-carboxyethyl)phosphine, tris(hydroxymethyl)aminomethane, potassium chloride, potassium ferricyanide and potassium hexacyanoferrate(II) were purchased from Sinopharm Chemical Reagent Co., Ltd. (Shanghai, China). Graphite oxide was purchased from Jicang Nano Tech Co., Ltd. (Nanjing, China). Polypropylene (PP) synthetic paper (5 mm in thickness) was purchased from Shengcai Packaging Products Co., Ltd. (Shanghai, China). Insulating ink (Jelcon AC-3 G) was purchased from Jujo Chemical Co., Ltd. (Japan). All thiol-modified aptamers and all-A sequences were synthesized by Sangon Biotechnology (Shanghai, China), and sequences are listed in Table 1 [31,32]. Ultrapure water (≥18 MΩ·cm) was generated by Millipore water purification system and used throughout the experiments.

2.2. Apparatus and measurements

The screen-printed carbon electrode (SPCE) was made with an AT-25 P instrument (Atma Champ Ent. Corp., China). Open circuit potential (OCP) measurements were performed with a CHI1030C electrochemical workstation (CH Instruments, Shanghai, China) and a two-electrode system consisting of the modified SPCE as the working electrode and a Ag/AgCl (filled with 3.0 M KCl) electrode as the reference electrode. Electrochemical impedance spectroscopy (EIS) measurements were carried out on a CHI660C electrochemical workstation (CH Instruments, Shanghai, China) with a conventional three-electrode system that was comprised of the modified SPCE as the working electrode, a platinum wire as the auxiliary electrode, and a Ag/AgCl electrode as the reference electrode. The determination of real samples was verified by an ABI6500 liquid chromatography-tandem mass spectrometer (Applied Biosystems Inc., Shanghai, China). The data fitting was performed with ZSimpWin software.

2.3. Fabrication of the aptasensor array

PP synthetic paper was used as the substrate for the four working channels. Silver paste was first printed as a conductive layer and was followed by printing with carbon paste. Then, the insulating paste was printed to define the area of the working channel (four circles on SPCE in Scheme 1). After each printing step, the electrodes needed to be vacuum-dried for 20 min at 100 °C, and then, an SPCE with four channels was finally obtained.

Reduced graphene oxide (rGO) was modified on the SPCE channels through electrochemical reduction in a N_2-purged dispersion solution (0.5 mg mL^{-1}) at a working potential of -0.8 V (vs. Ag/AgCl) for 600 s [33]. Afterward, a dendritic gold nanostructure-modified electrode was obtained by direct electrodeposition in a 2.8 mM $HAuCl_4$ and 0.1 M H_2SO_4 solution under a negative potential of -1.5 V for 600 s [34]. Then, 7 μL of two aptamer solutions and two internal calibration-DNA (IC-DNA) sequence solutions were self-assembled on the working area of the SPCE channels via Au-S bonds for 12 h at 25 °C. The unbound aptamers and DNA were removed by washing with 0.05 M Tris−HCl (pH = 7.4). After that, the aptasensor array was incubated in 2 mM 6-mercapto-1-hexanol (MCH) solution for ~1 h to block remaining active sites.

2.4. Simultaneous detection of streptomycin and kanamycin

Before recording the initial potentials, the aptasensor array was immersed in 0.05 M Tris−HCl (pH = 7.4) for 30 min to obtain stable OCP responses. Afterwards, this array was incubated with 3 mL of streptomycin and kanamycin mixture at different concentrations in 0.05 M Tris−HCl for 45 min at room temperature, which was followed by recording the final potentials of the four channels. Thus, the values of ΔOCP were obtained for further analysis.

Table 1
List of DNA sequences.

Name	Sequences
Streptomycin-aptamer	5′-SH-TAG GGA ATT CGT CGA CGG ATC CGG GGT CTG GTG TTC TGC TTT GTT CTG TCG GGT CGT CTG CAG GTC GAC GCA TGC GCC G-3′
Kanamycin-aptamer	5′-SH-AGA TGG GGG TTG AGG CTA AGC CGA-3′
Streptomycin-IC	5′-SH-AAA AAA AAA AAA AAA AAA AAA AAA AAA AAA AAA AAA AAA AAA AAA AAA AAA AAA AAA AAA AAA AAA AAA AAA AAA A-3′
Kanamycin-IC	5′-SH-AAA AAA AAA AAA AAA AAA AAA AAA-3′

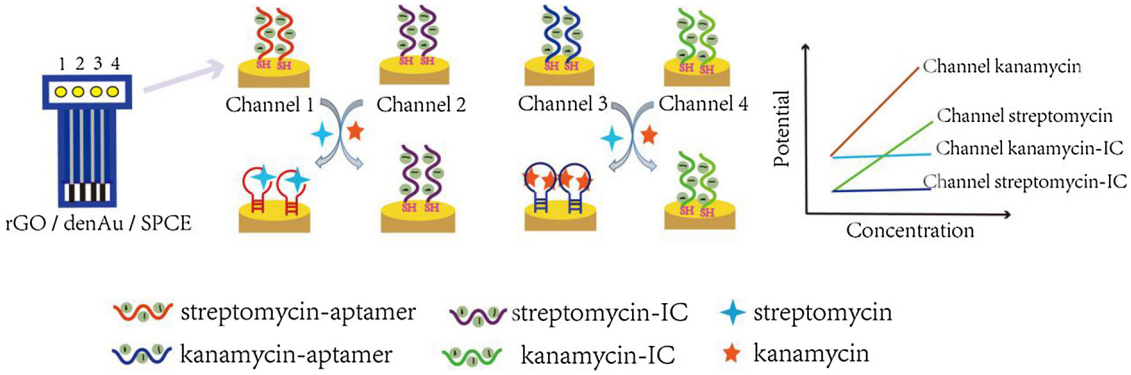

Scheme 1. Schematic illustration of the aptasensor for the simultaneous potentiometric detection of streptomycin and kanamycin with dual-channel internal calibration.

2.5. Determination of milk samples

Milk samples, purchased from a local supermarket, were mixed with quantitative standard streptomycin and kanamycin solutions and then used as artificially contaminated milk samples. For a pretreatment [35], acetic acid (20 %, v/v) was first added dropwise to the sample solution, generating a pH value of 4.7 to denature and precipitate the proteins in the milk at the isoelectric point. Subsequently, the sample was heated at 45 °C for 30 min to ensure that the casein was thoroughly precipitated. The pretreatment was followed by centrifugation at 11,000 rpm for 20 min to remove the precipitate, and then the sample was filtered with a 0.22 μm membrane. Finally, the potentiometric detection of streptomycin and kanamycin was carried out by the developed aptasensor array.

3. Results and discussion

3.1. Characterization of the aptasensor array

To confirm the successful fabrication of the aptasensor array, SEM and EIS were employed. As shown in Fig. 1A, the carbon layer is printed uniformly on the surface of the SPCE channels, thus providing a stable substrate. With the rGO modification, the surface becomes much smoother (Fig. 1B). The electrodeposition of denAu on the surface of rGO generates obvious dendritic nanostructures (Fig. 1C), which can effectively increase the area of the electrode surface.

EIS signals were collected to characterize the successful fabrication of the aptasensor array in a 5.0 mM $[Fe(CN)_6]^{4-}/[Fe(CN)_6]^{3-}$ solution containing 0.1 M KCl within a frequency range of 0.1 - 10^5 Hz (Fig. 1D). The inner illustration is the equivalent circuit diagram, consisting of the solution resistance (R_s), the charge transfer resistance between the electrode and the solution interface (R_{et}), the lipid bilayer capacitance (C_{dl}), constant phase angle element (Q) and inductance (L). The data fitting was performed with ZSimpWin software, as shown in Fig. S2. As previously reported [36], R_{et} can be deduced by the semicircle diameter of the Nyquist curve. Thus, it can be clearly observed that the bare SPCE channels show a relatively high resistance (curve a, $R_{et} \approx 2034\ \Omega$). The modification of the rGO membrane decreases the R_{et} value to ~1251 Ω (curve b), since its high conductivity and large surface area can facilitate electron transfer to the SPCE channel surface. With the following modification of denAu, the R_{et} value presents a drastic decrease (curve c, $R_{et} \approx 304.7\ \Omega$), which is attributed to the extended surface area and excellent conductivity of denAu. However, a significant increase in the R_{et} value is obtained after the self-assembly of the aptamers (curve d, $R_{et} \approx 3704\ \Omega$) because their weak conductivity inhibits electron transfer, indicating the successful aptamer modification.

3.2. Internal calibration

In potentiometric detection, the potential change is related not only to variations in the target but also to differences in the solution matrix. Therefore, it is especially necessary to calibrate the basic potential of the working electrode to improve the measurement accuracy. In this case, the integration of calibration channels shows its significance. To achieve the purpose of calibration, the initial potentials of the working and calibration channels should be the same [30]. It is known that the phosphate group of each nucleotide on the DNA/aptamer chain is negatively charged. When aptamers are fixed on the electrode, the initial potential of the electrode is determined by the amount of negative charges they carry, which depends on the number of nucleotides in the chain. Hence, a non-aptamer DNA sequence (all-A sequence) with the same number of nucleotides can be immobilized on the calibration channel and provide the same initial potential as the working channel. All-C, all-G, or all-T sequences will not affect the nature of the internal calibration, which has been verified in our previous work [30]. Since the aptamer lengths of the two targets, streptomycin and kanamycin, are quite different, it is improper to use one calibration DNA sequence as in our previous work; only one calibration sequence may affect the recognition capability of the aptamer to the target. Hence, two separate calibration channels are needed to ensure the accuracy of the target determination.

Fig. 2 shows the OCP responses of 4 channels before and after incubation with their corresponding targets. Clearly, the working channels and calibration channels present similar initial potentials without targets. The respective incubation with two targets generates obviously increased potentials due to the decreased negative charge density of the electrode surface, which is caused by the conformation change of the aptamers. However, the calibration channels only have slight changes because the non-aptamer sequences do not recognize the target. The changes are probably attributed to nonspecific adsorption. Consequently, it is necessary and feasible to introduce a dual-internal calibration system. The ΔOCP values of the aptasensors are calculated according to the following equation: $\Delta OCP = \Delta OCP_w - \Delta OCP_{IC}$, where ΔOCP_w and ΔOCP_{IC} represent the potential difference of the working channel and the calibration channel before and after binding to the target, respectively.

3.3. Evaluation of the cross-selectivity

To investigate the cross-selectivity of the 4 channels, 0.01 μM streptomycin and kanamycin were detected by the aptasensor array, respectively. As shown in Fig. S3, after incubation with streptomycin, only the potential of Channel streptomycin dramatically increased by 35.9 mV, while those of the other channels only varied by approximately 10 mV. Similarly, incubation with kanamycin increases the potential of Channel kanamycin by 43.6 mV, which is evidently higher

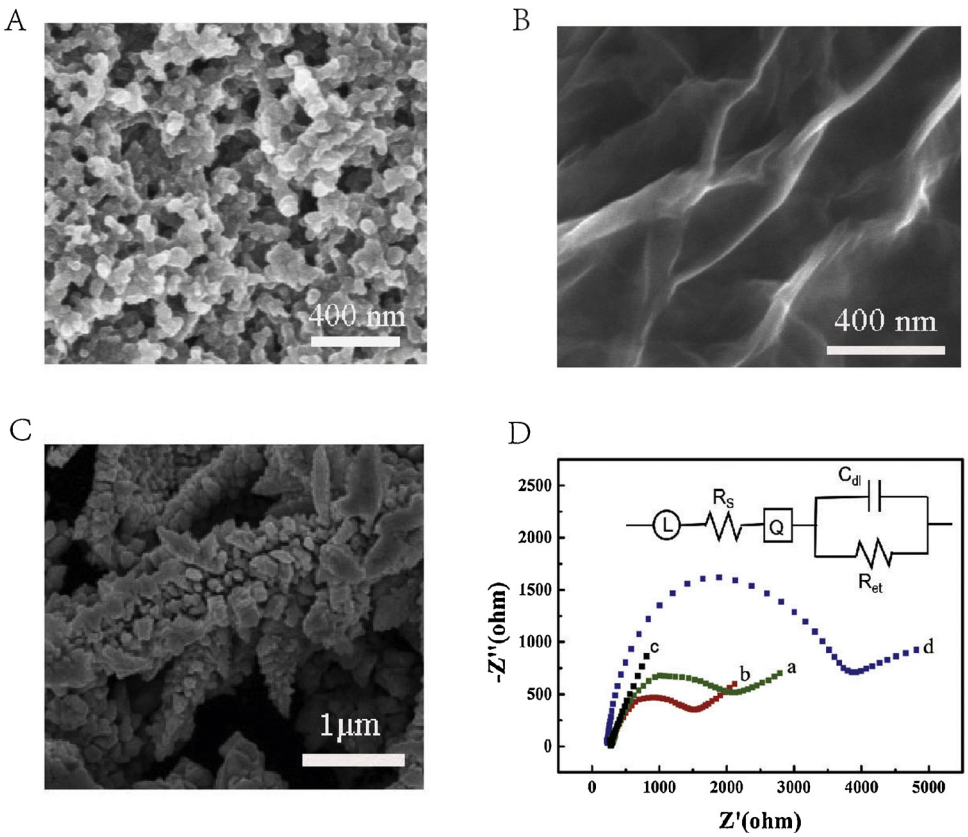

Fig. 1. SEM images of the (A) SPCE channels, (B) rGO/SPCE channels, and (C) denAu/rGO/SPCE channels. (D) EIS responses of the SPCE channels after each modification step in a 5.0 mM $[Fe(CN)_6]^{4-}/[Fe(CN)_6]^{3-}$ solution containing 0.1 M KCl: (a) bare SPCE channels, (b) rGO/SPCE channels, (c) denAu/rGO/SPCE channels, and (d) aptamer-modified denAu/rGO/SPCE channels.

than those of the other channels. Therefore, negligible interference exists between the two working channels, revealing the feasibility of simultaneously detecting streptomycin and kanamycin with this potentiometric aptasensor array.

3.4. Optimization of the experimental conditions

To achieve the best performance of the aptasensor array, three key parameters were optimized: the concentration of the two aptamers, the interaction time between the aptamers and the targets, and the pH value of the detection solution. Fig. 3A and 3D show the changes in potential responses with the increased concentration of the two aptamers. Clearly, the value of ΔOCP increases first and then remains almost the same. The increase in signal intensity is caused by more captured targets with the high concentrations of aptamers, but when the immobilized aptamers on the electrode surface reach saturation, the signal remains basically unchanged. Thus, the optimum concentrations of aptamer-streptomycin and aptamer-kanamycin were 3 μM and 2 μM, respectively.

Fig. 3B and 3E display the effect of the interaction time between the aptamers and the targets on the OCP responses. The ΔOCP value increases when the interaction time is extended from 20 to 45 min and then remains almost the same. Therefore, 45 min was selected as the optimal interaction time.

The pH value of the detection solution is another important factor influencing the performance of the aptasensor because it affects the structure and activity of the aptamer. The effect of the pH value was investigated in a range of 6.0 ~ 8.0 and is displayed in Fig. 3C and 3F. Obviously, the ΔOCP values present an increasing trend from 6.0 to 7.4 and then a decreasing trend from pH 7.4 to 8.0. Consequently, pH 7.4 was selected as the optimal pH value.

3.5. Simultaneous detection of streptomycin and kanamycin

Under optimal conditions, the mixed solution of streptomycin and kanamycin at different concentrations was determined by the

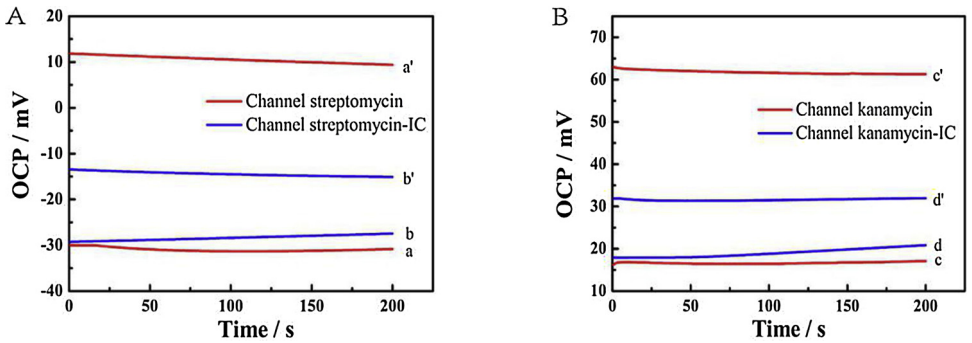

Fig. 2. OCP responses of (A) Channel streptomycin and Channel streptomycin-IC before (curves a and b) and after being incubated with 0.01 μM streptomycin for 45 min and (B) Channel kanamycin and Channel kanamycin-IC before (curves c and d) and after (curves c' and d') being incubated with 0.01 μM kanamycin for 45 min.

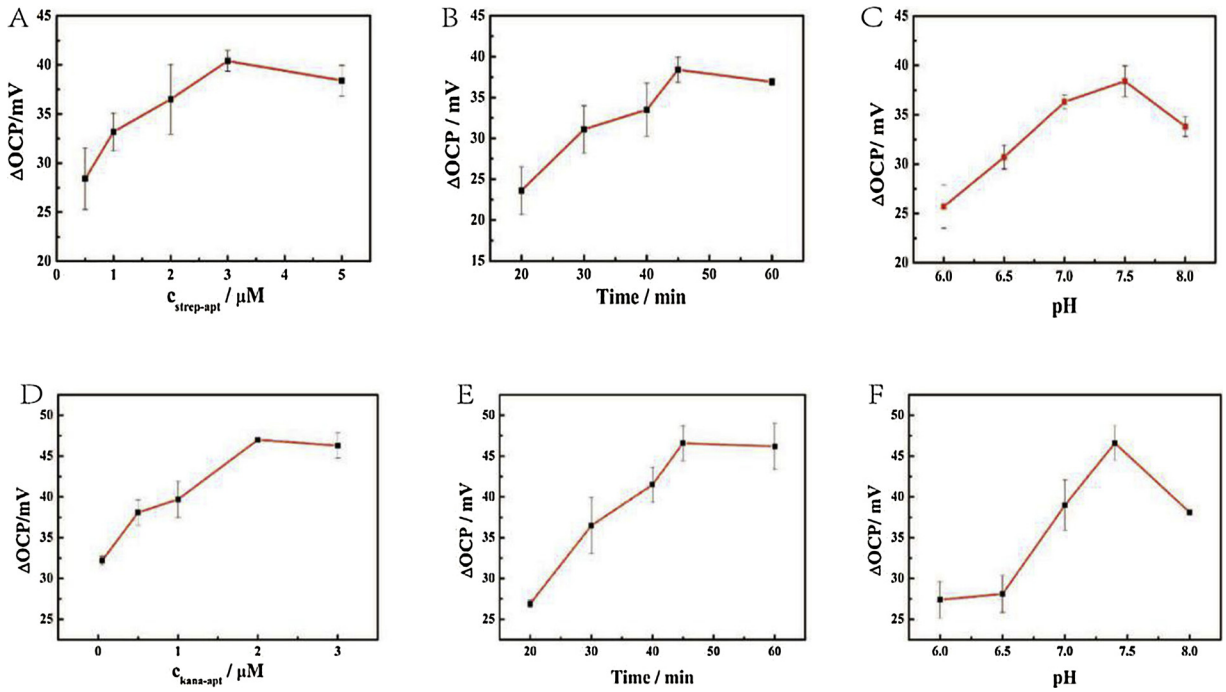

Fig. 3. Effect of (A) the concentration of aptamer-streptomycin, (B) interaction time between the aptamer and streptomycin, (C) pH value on the detection of streptomycin, (D) the concentration of aptamer-kanamycin, (E) interaction time between the aptamer and kanamycin, and (F) pH value on the detection of kanamycin. All determinations were performed in 0.05 M Tris − HCl solution containing 1 μM streptomycin and kanamycin. The error bars representing the standard deviation were derived from three determinations.

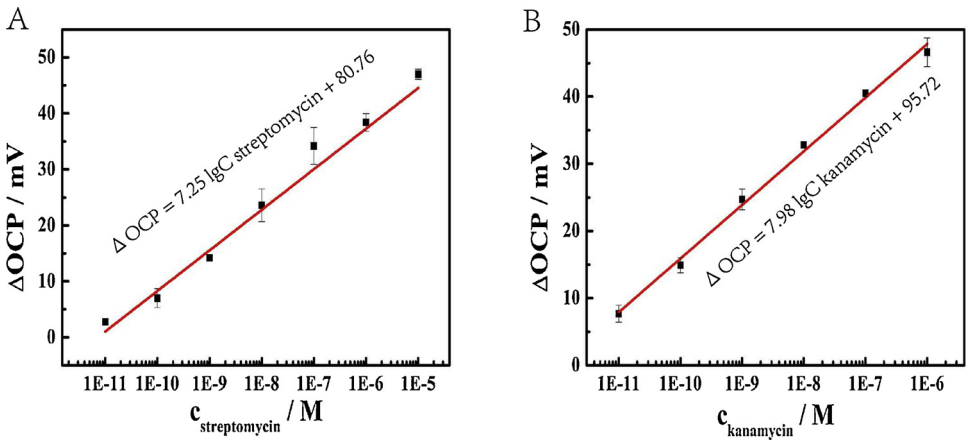

Fig. 4. Linear relationship between the ΔOCP values and the logarithm of the concentration for (A) streptomycin and (B) kanamycin. Error bars are the standard deviations across three repetitive measurements, and the data are fit using linear regression.

Table 2
Comparison of the determination methods for streptomycin.

Detection method	Detection limit	Detection range	Reference
Immunoassay	5 pg/mL (3.43 pM)	0.05 ~ 50 ng/mL (0.0343 ~ 34.3 nM)	[10]
Fluorimetry	54.5 nM	60 ~ 2060 nM	[13]
Colorimetry	94 nM	0.1 ~ 100 μM	[14]
High-performance liquid chromatography	6.8 nM	0.034 ~ 1.4 μM	[6]
Differential pulse voltammetry	36.45 pM	0.1 ~ 100 nM	[4]
This work	9.66 pM	10 pM–10 μM	–

potentiometric aptasensor array in 0.05 M Tris − HCl solution (pH = 7.4). Using the OCP responses of Channel IC for internal calibration, ΔOCP values were correlated to the concentrations of streptomycin and kanamycin. Thus, good linear relationships are established between the ΔOCP values and the logarithm of the target concentration, as shown in Fig. 4, and can be described as the following: $\Delta OCP = 7.25\lg C_{streptomycin} + 80.76$ ($R^2 = 0.9790$) in a range of 10 pM - 10 μM with a detection limit of 9.66 pM (S/N = 3, this concentration is obtained when the signal intensity of the target is three times that of the blank signal) and $\Delta OCP = 7.98\lg C_{kanamycin} + 95.72$ ($R^2 = 0.9950$) in a range of 10 pM - 1 μM with a detection limit of 5.24 pM (S/N = 3).

Moreover, the potential responses of the aptasensor array without

Table 3
Comparison of the determination methods for kanamycin.

Detection method	Detection limit	Detection range	Reference
Immunoassay	15 pg/mL (25.75 pM)	0.05 ~ 16 ng/mL (0.086 ~ 27.46 nM)	[11]
Fluorimetry	0.4 nM	1 ~ 50 nM	[12]
Colorimetry	2.6 ng/mL (4.46 nM)	0.05 ~ 0.6 μg/mL (0.086 ~ 1.03 μM)	[15]
High-performance liquid chromatography	25 nM	10 ~ 150 nM	[7]
Differential pulse voltammetry	74.50 pM	0.1 ~ 100 nM	[4]
This work	5.24 pM	10 pM–1 μM	–

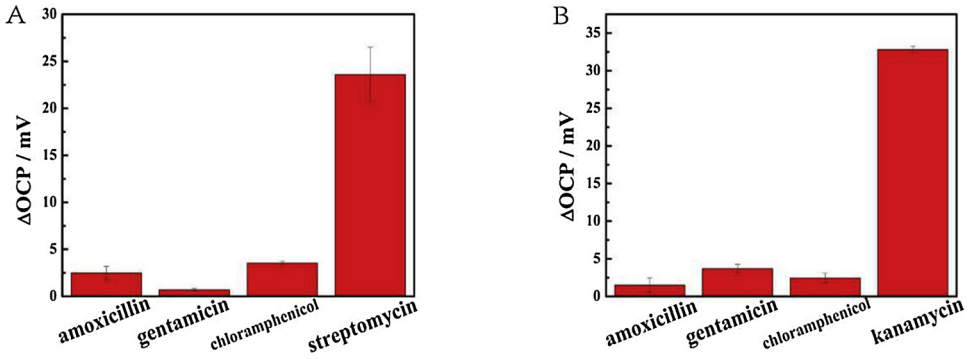

Fig. 5. Specificity of the aptasensor array for the detection of 0.01 μM (A) streptomycin and (B) kanamycin in the presence of 0.1 μM interferents, including chloramphenicol, gentamycin and amoxicillin. Error bars represent the standard deviations of three independent measurements.

Table 4
Repeatability of the aptasensor array.

Sample (1.00 nM)	Measured (nM)				Average value (nM)	RSD
	1	2	3	4		
Streptomycin	0.901	1.067	1.009	0.901	0.970	8.26 %
Kanamycin	0.885	0.962	0.962	0.861	0.918	5.23 %

internal calibration towards the two antibiotics at different concentrations were collected and are shown in Fig. S4. Obviously, without a calibration channel to provide a background response, the potential responses are much higher, while the response slopes are basically the same, indicating that the background matrix does affect the potential response but has little effect on the response slope. Therefore, the influence of the background matrix can be eliminated by the introduction of an internal calibration channel.

Furthermore, from the comparison of the analytical performance for streptomycin (Table 2) and kanamycin (Table 3) with other detection methods reported in recent years, it can be concluded that this aptasensor array exhibits a relatively wide linear range and a low detection limit; thus, its excellent performance and good application prospects are demonstrated.

3.6. Specificity and repeatability of the aptasensor array

Specificity is one of the most important characteristics of an aptasensor. To investigate the specificity of the aptasensor array, gentamicin, chloramphenicol, and amoxicillin were employed as interferents and detected by the aptasensor array. Fig. 5 shows that even if the concentration of interferents (0.1 μM) is 10 times higher than that of the targets (0.01 μM), the intensities of their potential responses are much lower than those of streptomycin or kanamycin. Consequently, the presence of these interferents shows almost no interference with the detection of the two targets, thus demonstrating good specificity.

Moreover, the specificity of the aptasensor array without an internal calibration channel was investigated, and the comparison results are shown in Fig. S5. It can be seen that without the calibration channel, the responses of the three interferents reach almost 30 % of the response of the target, showing that the introduction of the calibration channel can significantly improve the specificity of the aptasensor array.

The repeatability of the aptasensor array was also evaluated by detecting a mixed solution of streptomycin and kanamycin with the aptasensor arrays. As shown in Table 4, the calculated relative standard deviations (RSDs) of the four measurements are 8.26 % for streptomycin and 5.23 % for kanamycin, revealing the repeatable detection of streptomycin and kanamycin by the aptasensor array.

Table 5
Determination of streptomycin and kanamycin in milk samples.

Samples	Spiked streptomycin (mol/L)	Found streptomycin (mol/L)	Recovery (%)	RSD (%)	LC-MS (mol/L)
1	0.00	0.00	–	–	0.00
2	2.12×10^{-8}	1.93×10^{-8}	91.00	3.63	1.95×10^{-8}
3	7.06×10^{-8}	6.24×10^{-8}	88.36	8.74	6.91×10^{-8}
Samples	Spiked kanamycin (mol/L)	Found kanamycin (mol/L)	Recovery (%)	RSD (%)	LC-MS (mol/L)
1	0.00	0.00	–	–	0.00
2	5.30×10^{-8}	5.86×10^{-8}	110.63	7.79	4.54×10^{-8}
3	1.77×10^{-7}	1.91×10^{-7}	107.90	3.92	1.54×10^{-7}

3.7. Analysis of streptomycin and kanamycin in milk samples

To demonstrate the applicability of the potentiometric aptasensor array, streptomycin and kanamycin in primary and spiked milk samples were analysed by the proposed method. As shown in Table 5, the two targets cannot be detected in the primary milk sample, which is in accordance with national standards. In the two spiked samples, the recoveries of streptomycin are 91.00 % and 88.36 %, and the recoveries of kanamycin are 110.63 % and 107.90 %. The relative standard deviations (RSDs) of the measurements are 3.63 % and 8.74 % for streptomycin and 7.79 % and 3.92 % for kanamycin. Moreover, the obtained results are in good agreement with those measured by LC–MS, indicating that this aptasensor array provides a promising way to detect multiple antibiotics in real samples.

4. Conclusions

In this work, a simultaneous detection of streptomycin and kanamycin was realized using a potentiometric aptasensor array based on SPCE modified with rGO and denAu. To deduct the influence of the detection system on the potential variation of the working electrode and improve the detection accuracy, a dual-channel calibration system was introduced. The calibration system consisted of the immobilization of two DNA sequences with different lengths on the calibration channels, which provided the same initial potential as their corresponding working channels. Under optimal conditions, the ΔOCP values showed a linear correlation to the logarithmic concentration of streptomycin and kanamycin in a range of 10 pM–10 μM and 10 pM–1 μM, respectively, with detection limits of 9.66 pM and 5.24 pM, respectively. Moreover, this aptasensor array showed good specificity and repeatability and was successfully applied to the detection of streptomycin and kanamycin in milk samples. Therefore, the aptasensor array presents great potential for the on-site detection of multiple targets in the fields of food safety analysis, environmental monitoring and so on.

Declaration of Competing Interest

The authors declare that they have no known competing financial interests or personal relationships that could have appeared to influence the work reported in this paper.

Acknowledgement

This work was financially supported by the National Natural Science Foundation of China (Grant No. 21575042).

Appendix A. Supplementary data

Supplementary material related to this article can be found, in the online version, at doi:https://doi.org/10.1016/j.snb.2020.127857.

References

[1] X.Z. Wang, S.S. Dong, P.P. Gai, R. Duan, F. Li, Highly sensitive homogeneous electrochemical aptasensor for antibiotic residues detection based on dual recycling amplification strategy, Biosens. Bioelectron. 82 (2016) 49–54.
[2] N.M. Danesh, M. Ramezani, A.S. Emrani, K. Abnous, S.M. Taghdisi, A novel electrochemical aptasensor based on arch-shape structure of aptamer-complimentary strand conjugate and exonuclease I for sensitive detection of streptomycin, Biosens. Bioelectron. 75 (2016) 123–128.
[3] R.Y. Robati, A. Arab, M. Ramezani, F.A. Langroodi, K. Abnous, S.M. Taghdisi, Aptasensors for quantitative detection of kanamycin, Biosens. Bioelectron. 82 (2016) 162–172.
[4] F.L. Li, Y.M. Guo, X.Y. Wang, X. Sun, Multiplexed aptasensor based on metal ions labels for simultaneous detection of multiple antibiotic residues in milk, Biosens. Bioelectron. 115 (2018) 7–13.
[5] F.L. Li, X.Y. Wang, X. Sun, Y.M. Guo, Multiplex electrochemical aptasensor for detecting multiple antibiotics residues based on carbon fiber and mesoporous carbon-gold nanoparticles, Sens. Actuat. B Chem. 265 (2018) 217–226.
[6] B.J. Chen, H.Y. Zhang, B.X. Lin, J. Ge, L.H. Qiu, Determination of streptomycin residue in cucumber and Chinese cabbage by high-performance liquid chromatography with postcolumn derivatization and fluorometric detection, J. AOAC Int. 95 (2012) 523–527.
[7] B. Blanchaert, E. Podero´s Jorge, P. Jankovics, E. Adams, A.V. Schepdael, Assay of kanamycin A by HPLC with direct UV detection, Chromatographia 76 (2013) 1505–1512.
[8] A. Kaufmann, P. Butcher, K. Maden, Determination of aminoglycoside residues by liquid chromatography and tandem mass spectrometry in a variety of matrices, Anal. Chim. Acta 711 (2012) 46–53.
[9] A.M. Gremilogianni, N.C. Megoulas, M.A. Koupparis, Hydrophilic interaction vs ion pair liquid chromatography for the determination of streptomycin and dihydrostreptomycin residues in milk based on mass spectrometric detection, J. Chromatogr. A 1217 (2010) 6646–6651.
[10] B.Q. Liu, B. Zhang, Y.L. Cui, H.F. Chen, Z.Q. Gao, D.P. Tang, Multifunctional gold-silica nanostructures for ultrasensitive electrochemical immunoassay of streptomycin residues, ACS Appl. Mater. Interfaces 3 (2011) 4668–4676.
[11] S.J. Yu, Q. Wei, B. Du, D. Wu, H. Li, L.G. Yan, H.M. Ma, Y. Zhang, Label-free immunosensor for the detection of kanamycin using Ag@Fe_3O_4 nanoparticles and thionine mixed graphene sheet, Biosens. Bioelectron. 48 (2013) 224–229.
[12] Q.G. Liao, B.H. Wei, L.G. Luo, Aptamer based fluorometric determination of kanamycin using double-stranded DNA and carbon nanotubes, Microchim. Acta 184 (2016) 627–632.
[13] S.M. Taghdisi, N.M. Danesh, M.A. Nameghi, M. Ramezani, K. Abnous, A label-free fluorescent aptasensor for selective and sensitive detection of streptomycin in milk and blood serum, Food Chem. 203 (2016) 145–149.
[14] B.X. Lin, Y. Yu, Y.J. Cao, M.L. Guo, D.B. Zhu, J.X. Dai, M.S. Zheng, Point-of-care testing for streptomycin based on aptamer recognizing and digital image colorimetry by smartphone, Biosens. Bioelectron. 100 (2018) 482–489.
[15] Y.Y. Xu, T. Han, X.Q. Li, L.H. Sun, Y.J. Zhang, Y.S. Zhang, Colorimetric detection of kanamycin based on analyte-protected silver nanoparticles and aptamer-selective sensing mechanism, Anal. Chim. Acta 891 (2015) 298–303.
[16] E. Bakker, P. Bühlmann, E. Pretsch, Carrier-based ion-selective electrodes and bulk optodes. 1. General characteristics, Chem. Rev. 97 (1997) 3083–3132.
[17] Y. Yao, C.M. Jiang, J.F. Ping, Flexible freestanding graphene paper-based potentiometric enzymatic aptasensor for ultrasensitive wireless detection of kanamycin, Biosens. Bioelectron. 123 (2019) 178–184.
[18] J.W. Ding, B.W. Li, L.X. Chen, W. Qin, A three-dimensional origami paper-based device for potentiometric biosensing, Angew. Chem. Int. Ed. 55 (2016) 13033–13037.
[19] J.W. Ding, Y. Gu, F. Li, H.X. Zhang, W. Qin, DNA nanostructure-based magnetic beads for potentiometric aptasensing, Anal. Chem. 87 (2015) 6465–6469.
[20] A. Duzgun, A. Maroto, T. Mairal, C. O'Sullivan, F.X. Rius, Solid-contact potentiometric aptasensor based on aptamer functionalized carbon nanotubes for the direct determination of proteins, Analyst 135 (2010) 1037–1041.
[21] R. Hernandez, C. Valles, A.M. Benito, W.K. Maser, F.X. Rius, J. Riu, Graphene-based potentiometric biosensor for the immediate detection of living bacteria, Biosens. Bioelectron. 54 (2014) 553–557.
[22] R.N. Liang, J.W. Ding, S.S. Gao, W. Qin, Mussel-inspired surface-imprinted sensors for potentiometric label-free detection of biological species, Angew. Chem. Int. Ed. 56 (2017) 6833–6837.
[23] Y. Du, C.G. Chen, M. Zhou, S.J. Dong, E.K. Wang, Microfluidic electrochemical aptameric assay integrated on-chip: a potentially convenient sensing platform for the amplified and multiplex analysis of small molecules, Anal. Chem. 83 (2011) 1523–1529.
[24] M.R. Dunn, R.M. Jimenez, J.C. Chaput, Analysis of aptamer discovery and technology, Nat. Rev. Chem. 1 (2017) 76.
[25] A.B. Iliuk, L.H. Hu, W.A. Tao, Aptamer in bioanalytical applications, Anal. Chem. 83 (2011) 4440–4452.
[26] E.G. Lv, J.W. Ding, W. Qin, Potentiometric aptasensing of small molecules based on surface charge change, Sens. Actuators B Chem. 259 (2018) 463–466.
[27] G.A. Zelada-Guillen, J. Riu, A. Duzgun, F.X. Rius, Immediate detection of living bacteria at ultralow concentrations using a carbon nanotube based potentiometric aptasensor, Angew. Chem. Int. Ed. 48 (2009) 7334–7337.
[28] Y. Du, B.J. Lim, B.L. Li, Y.S. Jiang, J.L. Sessler, A.D. Ellington, Reagentless, ratiometric electrochemical DNA sensors with improved robustness and reproducibility, Anal. Chem. 86 (2014) 8010–8016.
[29] E.H. Xiong, X.H. Zhang, Y.Q. Liu, J.W. Zhou, P. Yu, X.Y. Li, J.H. Chen, Ultrasensitive electrochemical detection of nucleic acids based on the dual-signaling electrochemical ratiometric method and exonuclease III-assisted target recycling amplification strategy, Anal. Chem. 87 (2015) 7291–7296.
[30] W.X. Tang, Z.Z. Wang, J. Yu, F. Zhang, P.G. He, Internal calibration potentiometric aptasensors for simultaneous detection of Hg^{2+}, Cd^{2+}, and As^{3+} based on a screen-printed carbon electrodes array, Anal. Chem. 90 (2018) 8337–8344.
[31] N.D. Zhou, J.Y. Wang, J. Zhang, C. Li, Y.P. Tian, J. Wang, Selection and identification of streptomycin-specific single-stranded DNA aptamers and the application in the detection of streptomycin in honey, Talanta 108 (2013) 109–116.
[32] K.M. Song, M. Cho, H. Jo, K. Min, S.H. Jeon, T. Kim, M.S. Han, J.K. Ku, C. Ban, Gold nanoparticle-based colorimetric detection of kanamycin using a DNA aptamer, Anal. Biochem. 415 (2011) 175–181.
[33] J.F. Ping, Y.X. Wang, Y.B. Ying, J. Wu, Application of electrochemically reduced graphene oxide on screen-printed ion-selective electrode, Anal. Chem. 84 (2012) 3473–3479.
[34] F. Li, X.P. Han, S.F. Liu, Development of an electrochemical DNA biosensor with a high sensitivity of fM by dendritic gold nanostructure modified electrode, Biosens. Bioelectron. 26 (2011) 2619–2625.

[35] W. Yao, C.M. Jiang, J.F. Ping, Flexible freestanding graphene paper-based potentiometric enzymatic aptasensor for ultrasensitive wireless detection of kanamycin, Biosens. Bioelectron. 123 (2019) 178–184.
[36] L. Hou, Z.Q. Gao, M.D. Xu, X. Cao, X.P. Wu, G.N. Chen, D.P. Tang, DNAzyme-functionalized gold-palladium hybrid nanostructures for triple signal amplification of impedimetric immunosensor, Biosens. Bioelectron. 54 (2014) 365–371.

Juan Yu received a B.S. in Chemistry from Xinyang Normal University (Xinyang, China) in 2017. She is currently working towards her M.S. in Analytical Chemistry at East China Normal University (Shanghai, China). Her research interests is all-solid- state potentiometric aptasensing.

Wanxin Tang received her M.S. degree in Analytical Chemistry from Shanghai Normal University in 2015. Now she is preparing her Ph.D. degree at the School of Chemistry and Molecular Engineering in East China Normal University (Shanghai, China). Her research interests is solid-state potentiometric sensing and wearable electrochemical sensing technology.

Fan Wang received a M.S. in Material Physics & Chemistry from Shanghai University of engineering science (Shanghai, China) in 2018. She is currently working towards her Ph.D. in Analytical Chemistry at East China Normal University (Shanghai, China). Her research intetests is all solid-state ion selective electrode.

Fan Zhang received her M.S. in Analytical Chemistry from the Department of Chemistry at East China Normal University (Shanghai, China) in 2008. From 2008 to 2011, she worked as a jointly supervised Ph.D. student at the Department of Chemistry in Ecole Normale Supérieure (Paris, France) and East China Normal University (Shanghai, China). She is now working in the Department of Chemistry in East China Normal University (Shanghai, China) as an associate professor. Her research interests include the development of microfluidic devices and micro/nano electrodes and the study of electric and electrochemical responses of cells.

Qingjiang Wang received his Ph.D. degree in Analytical Chemistry at the Department of Chemistry in East China Normal University (Shanghai, China). Now he is working at School of Chemistry and Molecular Engineering in East China Normal University (Shanghai, China) as professor. His research interests include capillary electrophoresis, electrochemical biosensors and microfluidic chip electrophoresis.

Pingang He is the Vice Secretary-General of the Electrochemical Instrument Committee in the China Instrument and Control Society; the Director of the Analytical Chemistry Committee at the Shanghai Society of Chemistry and Chemical Industry; and the East China Normal University-Branch President of the Shanghai Overseas Returned Scholars Association. He received his Ph.D. from Fudan University (Shanghai, China) in 1996. Since 1998, he has been working as professor at East China Normal University (Shanghai, China). His research interests include biosensors, preparation and application of nanomaterials, electrochemistry/in situ electrochemistry of scanning probe, capillary electrophoresis/electrochemical detection, novel electrochemical analytical instrument.